Available online at www.sciencedirect.com
ScienceDirect
Nuclear Medicine and Biology 33 (2006) 945–952
NUCLEAR MEDICINE — AND — BIOLOGY
www.elsevier.com/locate/nucmedbio

[^{99m}Tc]HYNIC-RGD for imaging integrin $\alpha_v\beta_3$ expression

Clemens Decristoforo[a,*], Bluma Faintuch-Linkowski[b], Ana Rey[c], Elisabeth von Guggenberg[a], Marco Rupprich[a], Ignacio Hernandez-Gonzales[d], Teodoro Rodrigo[b], Roland Haubner[a]

[a]*Department of Nuclear Medicine, Medical University of Innsbruck, A-6020 Innsbruck, Austria*
[b]*Radiopharmacy Center Instituto de Pesquisas Energeticas e Nucleares (IPEN), 05508-900 São Paulo, Brazil*
[c]*Cátedra de Radioquímica, Facultad de Química, Universidad de la República, C.P. 11800 Montevideo, Uruguay*
[d]*Centro de Isotopos, Ciudad de la Habana, Cuba*

Received 9 June 2006; received in revised form 4 August 2006; accepted 2 September 2006

Abstract

There has been increasing interest in peptides containing the Arg–Gly–Asp (RGD) sequence for targeting of $\alpha_v\beta_3$ integrins to image angiogenesis. [^{18}F]Galacto-RGD has been successfully used for positron emission tomography applications in patients. Here we report on the preclinical characterization of a ^{99m}Tc-labeled derivative for single-photon emission computed tomography.

c(RGDyK) was derivatized with HYNIC at the ε-amino group of the lysine [c(RGDyK(HYNIC)) or HYNIC-RGD]. ^{99m}Tc labeling was performed using coligands (tricine and EDDA), as well as $^{99m}Tc(CO)_3(H_2O)_3$. Radiolabeled peptides were characterized with regard to lipophilicity, protein binding and stability in buffer, serum and tissue homogenates. Integrin receptor activity was determined in internalization assays using $\alpha_v\beta_3$-receptor-positive M21 and $\alpha_v\beta_3$-receptor-negative M21L melanoma cells. Biodistribution was evaluated in normal and nude mice bearing M21, M21L and small cell lung tumors.

HYNIC-RGD could be labeled at high specific activities using tricine, tricine–trisodium triphenylphosphine 3,3′,3″-trisulfonate (TPPTS), tricine–nicotinic acid (NA) or EDDA as coligands. [^{99m}Tc]EDDA/HYNIC-RGD, [^{99m}Tc]tricine–TPPTS/HYNIC-RGD and [^{99m}Tc]tricine–NA/HYNIC-RGD showed protein binding (<5%) considerably lower than [^{99m}Tc](CO)$_3$-HYNIC-RGD and [^{99m}Tc]tricine/HYNIC-RGD. [^{99m}Tc]EDDA/HYNIC-RGD revealed high in vitro stability accompanied by low lipophilicity with a log P value of −3.56, comparable to that of [^{18}F]Galacto-RGD. In M21 cells for this compound, the highest level of specific and rapid cell uptake (1.25% mg protein^{-1}) was determined. In vivo, rapid renal excretion, low blood retention, low liver and muscle uptakes and low intestinal excretion 4 h postinjection were observed. Tumor uptake values were 2.73% ID/g in M21 $\alpha_v\beta_3$-receptor-positive tumors versus 0.85% ID/g in receptor-negative tumors 1 h postinjection. Small cell lung tumors could be visualized using γ camera imaging.

[^{99m}Tc]EDDA/HYNIC-RGD shows encouraging properties to target $\alpha_v\beta_3$ receptors in vivo with high stability and favorable pharmacokinetics. Tumor uptake studies showed specific targeting of $\alpha_v\beta_3$-receptor-positive tumors with tumor-to-organ ratios comparable to those of [^{18}F]Galacto-RGD.

Keywords: RGD; Technetium-99m; HYNIC; $\alpha_v\beta_3$

1. Introduction

Radiolabeled peptides, such as somatostatin, gastrin-releasing peptide and gastrin analogues, have been successfully used to image G-protein-coupled receptors in tumor patients [1]. This success is based on high affinity for the target receptor, good internalization and retention in cells and rapid predominant renal excretion from nontarget tissues [2]. However, the use of these peptides is limited by great differences in the expression of those regulatory peptide receptors in tumor tissues [3].

Recently there has been interest in targeting integrin receptors for in vivo tumor imaging [4]. Especially integrin $\alpha_v\beta_3$, which mediates binding to the extracellular matrix via a variety of different proteins (e.g., vitronectin, fibronectin

* Corresponding author. Universitaetsklinik fuer Nuklearmedizin, Anichstrasse 35, A-6020 Innsbruck, Austria. Tel.: +4351250480951; fax: +4351250422659.
E-mail address: clemens.decristoforo@uibk.ac.at (C. Decristoforo).

0969-8051/$ – see front matter © 2006 Elsevier Inc. All rights reserved.
doi:10.1016/j.nucmedbio.2006.09.001

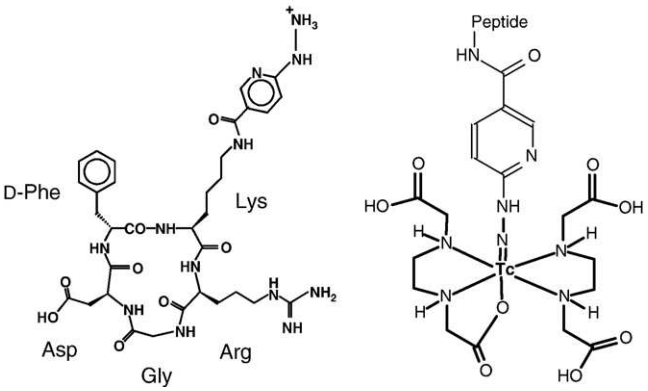

Fig. 1. Structure of HYNIC-RGD (cyclo[Arg–Gly–Asp–D-Tyr–(Lys-HYNIC)]) and the proposed ^{99m}Tc complex using EDDA as coligand.

and von Willebrand factor), is a target structure for the development of this new class of radiopharmaceuticals. This integrin is involved in different pathological processes, such as tumor metastasis and tumor-induced angiogenesis, restenosis, osteoporosis and inflammatory processes [5]. For example, several studies have shown that there is a correlation between $\alpha_v\beta_3$ expression and the metastatic potential of the corresponding tumor [6]. Moreover, this integrin is expressed on activated endothelial cells during migration through the basement membrane in the angiogenic process. Thus, several approaches have focused on the inhibition of tumor-induced angiogenesis via the targeting of this receptor. Development of inhibitors is based on peptides containing the amino acid sequence Arg–Gly–Asp (RGD), which is found to be essential in the binding of a variety of extracellular matrix proteins. The cyclic pentapeptide c(RGDfV) [7] has been proven to be selective for integrin $\alpha_v\beta_3$ and, thus, is used as a lead structure for tracer development [8]. Meanwhile, RGD peptides labeled with ^{111}In, ^{90}Y, ^{99m}Tc, ^{123}I, ^{64}Cu and ^{18}F have been introduced [4,5]. Most of them show high $\alpha_v\beta_3$ affinity in vitro and allow targeting of receptor-positive tumors in vivo. Major differences are found in the pharmacokinetics of different tracers. The most intensively studied compound yet is [^{18}F]Galacto-RGD, which allows noninvasive determination of $\alpha_v\beta_3$ expression not only in murine tumor models but also in tumor patients [9].

However, ^{99m}Tc labeling is still an attractive approach for radiolabeling peptides for single-photon emission computed tomography (SPECT) imaging, and a number of labeling technologies have been successfully used in patients [10]. Our group has shown that the use of the HYNIC approach is suitable for radiolabeling peptides with high specific activity, resulting in suitable pharmacokinetics for imaging purposes [11,12].

Here we describe the radiolabeling of a HYNIC-derivatized monomeric RGD peptide [c(RGDyK(HYNIC)) or HYNIC-RGD; Fig. 1] and its in vitro and in vivo evaluation for targeting the $\alpha_v\beta_3$ receptor in vivo.

2. Materials and methods

2.1. Materials

Reagents were purchased from Aldrich-Sigma Chemical Co., except when otherwise stated, and used as received.

HYNIC-RGD (cyclo[Arg–Gly–Asp–D-Tyr–(Lys-HYNIC)]; HYNIC=2-hydrazinonicotinic acid) and c(RGDyK) were synthesized on solid support using standard F-moc solid-phase chemistry (Biosynthan, Berlin, Germany) with a purity of >95%, as analyzed by reverse-phase high-performance liquid chromatography (RP-HPLC) and mass spectroscopy (MS).

[^{125}I]Echistatin was purchased from Amersham Life Science (Boston, MA).

$Na^{99m}TcO_4^-$ was obtained from a commercial ^{99}Mo/^{99m}Tc generator (ULTRATECHNEKOW, Mallinckrodt, The Netherlands).

2.2. Analytical methods

2.2.1. HPLC

A Dionex P680 low-pressure gradient pump with a Spectra Physics Spectra Chrom 100 variable UV detector and a Bioscan radiometric detector was used for RP-HPLC analysis. A Bischof Nucleosil 100-5 C_{18} 250×4.6-mm column, at a flow rate of 1 ml/min and with UV detection at 220 nm, was employed with the following gradients: Method 1: ACN/0.1% TFA/H_2O: 0–1.5 min, 0% ACN; 1.5–18 min, 0–30% ACN; 18–21 min, 30–60% ACN; 21–24 min, 60% ACN.

2.3. ^{99m}Tc labeling

2.3.1. Tricine as coligand

In a rubber-sealed vial, 5 μg of HYNIC-RGD was incubated with 0.5 ml of tricine solution (70 mg/ml in water), 0.5 ml of $^{99m}TcO_4^-$ solution (>200 MBq) and 20 μl of tin(II) solution (10 mg of $SnCl_2 \cdot 2H_2O$ in 10 ml of nitrogen-purged 0.1 N HCl) for 20 min at room temperature.

2.3.2. Tricine ternary coligands

Nicotinic acid (NA) and trisodium triphenylphosphine 3,3′,3″-trisulfonate (TPPTS) were used as ternary coligands. In a rubber-sealed vial, 5 μg of HYNIC-RGD was heated with 0.5 ml of tricine solution (70 mg/ml in water), 0.5 ml of $^{99m}TcO_4^-$ solution (>200 MBq), 20 μl of tin(II) solution (10 mg of $SnCl_2 \cdot 2H_2O$ in 10 ml of nitrogen-purged 0.1 N HCl) and 0.1 ml of NA solution (40 mg/ml in water) or 0.2 ml of TPPTS solution (5 mg/ml in water) for 15 min 100°C (NA) or for 30 min at 50°C (TPPTS).

2.3.3. Tricine–EDDA exchange labeling

In a rubber-sealed vial, 10 μg of HYNIC-RGD was incubated with 1 ml of EDDA/tricine solution (20 mg/ml tricine, 10 mg/ml EDDA in pH 6–7), 1 ml of $^{99m}TcO_4^-$ solution (800 MBq) and 20 μl of tin(II) solution (10 mg of

$SnCl_2 \cdot 2H_2O$ in 10 ml of nitrogen-purged 0.1 N HCl) for 10 min at 100°C.

2.3.4. Tc carbonyl

Carbonyl aquaion $[^{99m}Tc(OH_2)_3(CO)_3]^+$ was prepared from a commercial kit (ISOLINK, Mallinckrodt, Petten) according to the manufacturer's instructions (1 ml volume; 200–1000 MBq ^{99m}Tc). Five or 20 μg of peptide HYNIC-RGD was incubated with 100 μl of $[^{99m}Tc(OH_2)_3(CO)_3]^+$ labeling solution (up to 400 MBq) for 30 min at 70°C.

2.4. In vitro evaluation of radiolabeled peptides

2.4.1. Stability

The stability of radiolabeled peptides in aqueous solution was tested by the incubation of the reaction mixture purified by solid-phase extraction (SPE) using a SEPPAK C_{18} cartridge (Waters, USA) at a concentration of 200–1000 pmol/ml peptide in phosphate buffer, as well as in a solution containing 10,000-fold molar excess of cysteine or histidine compared to the peptide at pH 7.4 at 37°C up to 24 h. Stability in fresh human plasma, as well as in kidney and liver homogenates, was measured in parallel. After incubation, plasma samples were precipitated with acetonitrile and centrifuged (1750×*g*, 5 min). Degradation of ^{99m}Tc complexes was assessed by HPLC. For incubation in kidney and liver homogenates, kidneys or livers freshly excised from rats were rapidly rinsed and homogenized in 20 mM HEPES buffer (pH 7.3) with an Ultra-Turrax T25 homogenator for 1 min at room temperature. Radiopeptides were incubated with fresh 30% homogenate at a concentration of 250–500 pmol/ml peptide at 37°C up to 2 h. Samples were precipitated with acetonitrile, centrifuged (1750×*g*, 5 min) and analyzed by HPLC.

2.4.2. Protein binding

For protein-binding assessment, SPE-purified complexes were incubated at a concentration of 20–100 pmol/ml peptide in fresh human plasma at 37°C and analyzed by size exclusion chromatography (MicroSpin G-50 Columns; Sephadex G-50) up to 6 h. Protein binding of the ^{99m}Tc complex was determined by measuring columns and eluates in a γ counter (Compugamma LKB, Finland).

2.4.3. Log P values

^{99m}Tc-labeled HYNIC-RGD (0.5 ml) in phosphate-buffered saline (PBS) was added to 0.5 ml of octanol in an Eppendorf vial. The tube was vigorously vortexed over a period of 15 min and centrifuged at 5000×*g* for 3 min. A 100 μl aliquot of both aqueous and octanol layers was collected and counted in a γ counter, and log *P* values were calculated.

2.4.4. Binding affinity

The in vitro binding affinity of HYNIC-RGD was determined in comparison with that of c(RGDfV) using [^{125}I]Echistatin as radioligand. [^{125}I]Echistatin was purchased from Amersham-Pharmacia Biotech (Vienna, Austria), and $\alpha_v\beta_3$ integrin receptors were from Chemicon (Temecula, CA). Briefly, 96-well plates were coated with $\alpha_v\beta_3$ integrin receptors and incubated with a mixture of [^{125}I]echistatin and varying concentrations of the peptide. Unbound radioligand was removed, and wells were washed. Bound radioligand was removed with 2 N NaOH. IC_{50} was calculated by fitting percent inhibition values using ORIGIN software (Northampton, MA).

2.5. Internalization and binding studies in $\alpha_v\beta_3$-positive and $\alpha_v\beta_3$-negative cells

$\alpha_v\beta_3$-Positive M21 and $\alpha_v\beta_3$-negative M21L human melanoma cells were grown in culture until a sufficient number of cells were available. For internalization experiments, cells were collected up to a concentration of 2×10^6 cells/ml in RPMI 1640 containing 1% glutamine and 1% PBS. Each 1 ml was pipetted into a separate tube. After the addition of ^{99m}Tc-labeled peptide (>100,000 cpm, 1 nM), cells were incubated at 37°C for 90 min in triplicate with either PBS/0.5% BSA buffer alone (150 μl, total series) or with 10 μM c(RGDyK) in PBS/0.5% BSA buffer (150 μl, nonspecific series). Incubation was interrupted by centrifugation, removal of medium and rapid rinsing with ice-cold Tris-buffered saline twice. Thereafter, the cells were incubated twice at room temperature in acid wash buffer (50 mM acetate buffer, pH 4.2) for 15 min at 37°C. The supernatant was collected (membrane-bound radioligand fraction), and the cells were washed with acid wash buffer. Cells were lysed by treatment in 1 N NaOH, and cell radioactivity was measured (internalized radioligand fraction). Protein concentration in NaOH fraction was determined using spectrophotometric determination (Bredford Assay, Sigma Aldrich Chemical Co.). Internalized and noninternalized fractions were determined by measuring radioactivity, and internalized fraction was expressed as the percentage of total activity per milligram of protein.

2.6. In vivo evaluation of radiolabeled peptides

All animal experiments were conducted in compliance with Austrian animal protection laws and with the approval of the Austrian Ministry of Science.

2.6.1. Human melanoma model

Tumor uptake studies were performed in male nu/nu mice (Charles River, Germany). For the induction of tumor

Table 1
In vitro data as determined for all ^{99m}Tc-labeled HYNIC-RGD conjugates

Compound	t_R (min)	Log *P* O/W	Labeling yield (*n*=3) (%)
[^{99m}Tc]EDDA/HYNIC-RGD	16.5	−3.57	93.9
[^{99m}Tc]Tricine/HYNIC-RGD	16.3	−3.75	99.5
[^{99m}Tc]Tricine–NA/HYNIC-RGD	17.1	−3.53	99.8
[^{99m}Tc]Tricine–TPPTS/HYNIC-RGD	15.2	−4.53	99.7
[^{99m}Tc](CO)$_3$/HYNIC-RGD	19.3	−1.69	99.6

O/W, octanol/water.

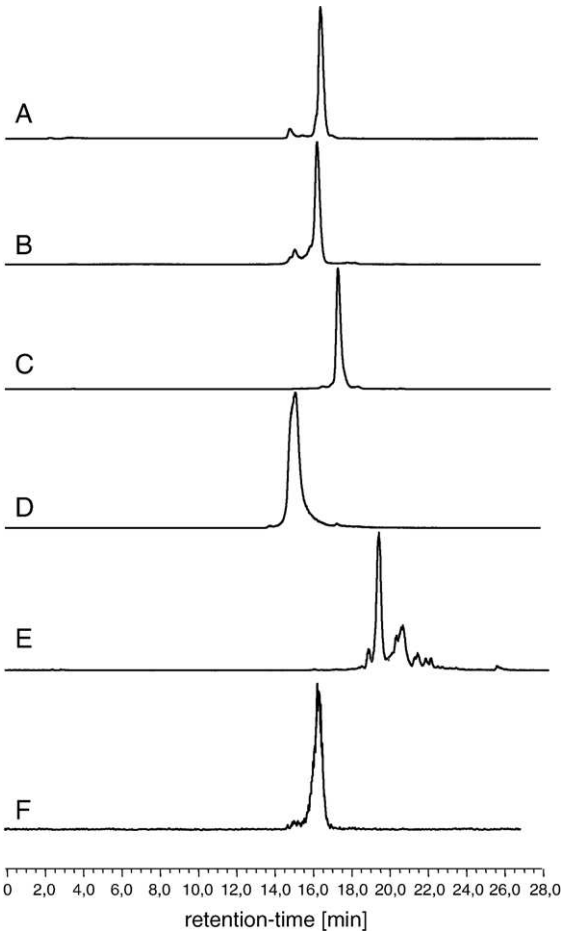

Fig. 2. Radiochromatograms: (A) [^{99m}Tc]EDDA/HYNIC-RGD; (B) [^{99m}Tc]tricine/HYNIC-RGD; (C) [^{99m}Tc]tricine–NA/HYNIC-RGD; (D) [^{99m}Tc]tricine–TPPTS/HYNIC-RGD; (E) [^{99m}Tc](CO)$_3$/HYNIC-RGD; (F) [^{99m}Tc]EDDA/HYNIC-RGD in liver homogenates at 2 h.

xenografts, M21 and M21L cells were subcutaneously injected at a concentration of 5×10^6 cells/mouse and allowed to grow until tumors of 0.3–0.6 ml were visible. On the day of the experiment, each of the six mice with M21 tumors and three mice with M21L tumors were injected with [^{99m}Tc]EDDA/HYNIC-RGD (1 MBq/mouse, corresponding to 1 μg of peptide) intravenously into the tail vein. They were sacrificed by cervical dislocation 1 h (M21 and M21L) or 4 h postinjection (M21).

Tumors and normal tissues (blood, lung, heart, stomach, spleen, liver, pancreas, kidneys, muscle and intestines) were removed. The amount of radioactivity was determined using a γ counter. Results were expressed as the percentage of injected dose per gram of tissue (% ID/g), and tumor-to-organ ratios were calculated.

2.6.2. Non small cell lung cancer model

A549 cells, a human non small cell lung carcinoma cell line, were grown to confluency and then harvested by trypsinization. After centrifugation for 5 min at $1000\times g$, the cells were resuspended in PBS. Male nu/nu mice were injected subcutaneously on the right upper back with a suspension of 6.5×10^6 cells. Tumor-bearing mice were used in biodistribution and imaging studies. For biodistribution, mice were injected, sacrificed and dissected as described above. Results were expressed as the percentage of injected dose per gram of tissue, and tumor-to-organ ratios were calculated.

Planar γ camera imaging was performed with a mobile scintillation camera (LEM Siemens) equipped with a 4.0-mm pinhole collimator. A syringe with a known amount of radioactivity was scanned, along with the mice, to allow semiquantification of the results using region-of-interest (ROI) analysis. All animals were injected intravenously with 0.1 ml (37 MBq, 1 μg of peptide) of [^{99m}Tc]EDDA/HYNIC-RGD, with and without excess c(RGDyK) (100 μg) in 0.9% saline, via the lateral tail vein. Four hours postinjection, the animals were anesthetized by intraperitoneal injection with urethane solution. A total of 500,000 counts were obtained per projection, under a 64×64 matrix. Ten-minute images of 60 s were acquired, which were drawn later using magnetic resonance imaging maximum intensity projection.

3. Results

HYNIC-RGD could be labeled at high specific activities (100 GBq/μmol) using EDDA, tricine, tricine–NA or tricine–TPPTS as coligands, resulting in a single major species as analyzed by HPLC. Corresponding data are summarized in Table 1. Mean labeling yields ($n=3$) were 93.9% for [^{99m}Tc]EDDA/HYNIC-RGDyK and >99% for other coligands. Labeling using carbonyl aquaion [^{99m}Tc$(OH_2)_3(CO)_3$] also resulted in high labeling yields (99.6%; $n=3$), but multiple species with a retention time significantly higher than the main peak ($t_R=19.3$ min) were detected (representative chromatograms of all ^{99m}Tc-labeled peptides are shown in Fig. 2).

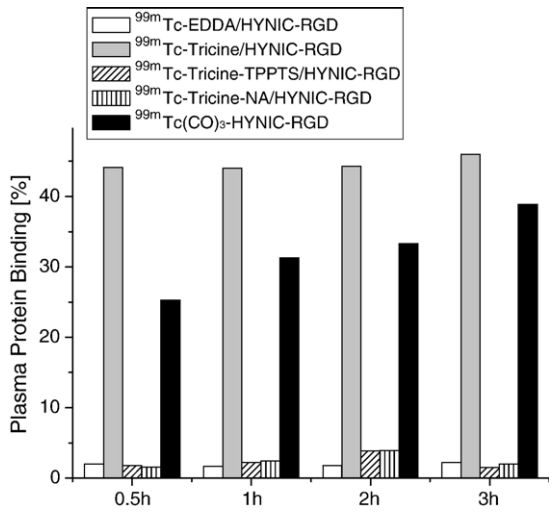

Fig. 3. Plasma protein binding of [^{99m}Tc]HYNIC-RGD derivatives under study.

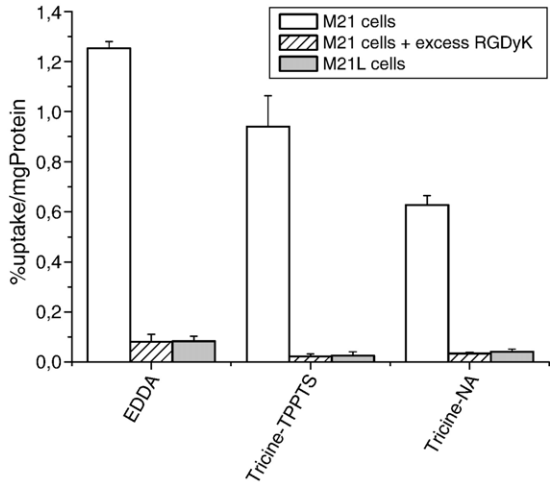

Fig. 4. Cell uptake of [^{99m}Tc]HYNIC-RGD using various coligands in $\alpha_v\beta_3$-integrin-receptor-positive M21 melanoma and receptor-negative M21L cells (blocked: coincubation with 10 μM RGD).

Stability studies in buffer, cysteine solution, human plasma or tissue homogenates revealed a high stability of all complexes prepared, with no significant release of radiolabel or peptide degradation during the observation period (for [^{99m}Tc]EDDA/HYNIC-RGD in liver homogenates, see also Fig. 2).

Protein-binding values are shown in Fig. 3. Very low levels of protein binding (<5% after 3 h incubation) were found using EDDA, tricine–TPPTS and tricine–NA as coligands, whereas high levels above 40% were determined for tricine as coligand. HYNIC-RGD labeling using the $Tc(CO)_3$ core revealed 25.3% protein binding after 30 min, increasing to 38.9% after 3 h. All ^{99m}Tc-labeled HYNIC-RGD conjugates revealed a higher hydrophilicity, with a log *P* value of <-3.5 compared to -3.2 of [^{18}F]Galacto-RGD, except $^{99m}Tc(CO)_3$/HYNIC-RGD; log *P* values correlated with HPLC retention times (see Table 1). A high binding affinity to $\alpha_v\beta_3$ integrin was determined for HYNIC-RGD with an IC_{50} value of 6.0 nM, in comparison to c(RGDfV) with an IC_{50} value of 3.7 nM in the same assay. Uptake in $\alpha_v\beta_3$-receptor-positive M21 melanoma cells for [^{99m}Tc]EDDA/HYNIC-RGD, [^{99m}Tc]tricine–TPPTS/HYNIC-RGD and [^{99m}Tc]tricine–NA/HYNIC-RGD is shown in Fig. 4. Cellular uptake for [^{99m}Tc]HYNIC-RGD declined in the series EDDA (1.25% mg protein^{-1})> tricine–TPPTS (0.94% mg protein^{-1})>tricine–NA (0.63% mg protein^{-1}). For all compounds, uptake could be reduced to <0.1% mg protein^{-1} by incubating with excess c(RGDyK). A comparably low uptake (<0.1% mg protein^{-1}) was found for receptor-negative M21L cells. Based on these results, [^{99m}Tc]EDDA/HYNIC-RGD was chosen for further in vivo evaluation in $\alpha_v\beta_3$-receptor-positive and $\alpha_v\beta_3$-receptor-negative tumor-bearing mice.

Table 2
Biodistribution of [^{99m}Tc]EDDA/HYNIC-RGD in Balb/c nude mice carrying $\alpha_v\beta_3$-positive tumors (M21) 1 and 4 h postinjection and $\alpha_v\beta_3$-negative tumors (M21L) 1 h postinjection

Organ	M21	M21	M21L
	1 h	4 h	1 h
Blood	0.98±0.04	0.45±0.02	1.27±0.16
Heart	1.01±0.05	0.64±0.09	1.00±0.05
Stomach	2.50±0.75	1.28±0.22	2.68±0.67
Liver	2.63±0.14	1.71±0.28	2.43±0.11
Kidneys	3.68±0.13	2.81±0.37	3.44±0.10
Muscle	0.76±0.69	0.34±0.05	0.54±0.10
Intestine	2.04±0.18	1.29±0.25	1.82±0.01
Tumor	2.73±0.26	2.06±0.37	0.85±0.20

Table 3
Biodistribution of [^{99m}Tc]EDDA/HYNIC-RGD in Balb/c nu/nu mice carrying A549 tumors with tumor-to-organ ratios in comparison with normal mice 4 h postinjection

Organ	A549	Tumor-to-organ ratio	Normal
Blood	0.08±0.02	19.25	0.07±0.03
Heart	0.43±0.09	3.58	0.41±0.04
Stomach	1.39±0.06	1.11	1.12±0.13
Liver	1.45±0.09	1.06	1.53±0.25
Kidneys	2.61±0.12	0.59	2.45±0.15
Muscle	0.20±0.01	7.70	0.27±0.02
Small intestine	1.36±0.02	1.13	1.57±0.02
Large intestine	1.83±0.07	0.84	1.48±0.12
Tumor	1.54±0.28	1.00	NA

Biodistribution data in the M21 and M21L tumor models are summarized in Table 2. Overall, a rapid almost exclusive elimination via the renal pathway could be observed with retention in all organs lower than 4% ID/g after 1 h and lower than 3% ID/g after 4 h. The highest values were found in the kidneys, with 3.67% versus 2.81% (1 vs. 4 h). Uptake in the liver and intestines was low, with 2.62% and 2.04% after 1 h and with 1.71% and 1.28% after 4 h, respectively; blood levels of 0.97% at 1 h and 0.45% after 4 h indicate moderate retention in the circulation. Tumor uptake values

Fig. 5. Planar γ camera images of [^{99m}Tc]EDDA/HYNIC-RGD in A549 tumor-bearing mice 4 h postinjection, without (left) and with (right) blocking receptors, by coinjection of 100 μg of c(RGDyK). Tumors on the left upper quadrant of the back are clearly delineated. Uptake, as calculated with ROI technique, was 4.92% (left; unblocked) and 0.88% (right; blocked), respectively, showing receptor-specific uptake in the tumor. The main activity is shown in the bladder, indicating predominant renal excretion.

of 2.72% and 2.06% after 1 and 4 h, respectively, indicate good uptake and retention. This uptake was shown to be specific as receptor-negative M21L tumor-bearing mice showed a significantly ($P<.05$) lower value of 0.85%; in none of the organs was any significant difference between M21 and M21L tumor observed.

Results of a comparative study in nude mice carrying a human small cell lung cancer with normal mice are summarized in Table 3. Both in normal and in A549 tumor-bearing mice, the organ with the highest tracer uptake was the kidney. Intestinal excretion and liver uptake were low. Tracer uptake in the tumor reached 1.5% 4 h postinjection. Comparative imaging in two A549 tumor-bearing mice with and without coinjection of excess c(RGDyK) for receptor blockade is shown in Fig. 5. The predominant renal excretion pathway is clearly seen with high activity values in the bladder, whereas liver uptake and kidney retention are low. The tumor is clearly delineated, and uptake as calculated from ROI technique was 4.92% (unblocked) and 0.88% (blocked), respectively, showing receptor-specific uptake in the tumor.

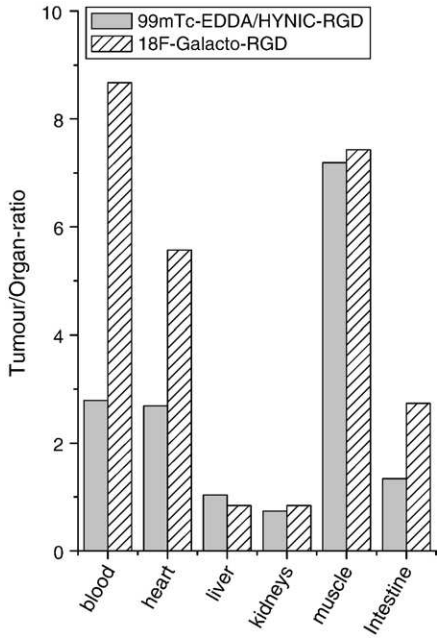

Fig. 6. Tumor-to-organ ratios of [^{99m}Tc]EDDA/HYNIC-RGD in comparison with [^{18}F]galacto-RGD in a $\alpha_v\beta_3$-receptor-positive nude mouse M21 human melanoma tumor model.

4. Discussion and conclusion

We attempted to label a peptide targeting the $\alpha_v\beta_3$ integrin with ^{99m}Tc for potential imaging of tumors and tumor-induced angiogenesis. Technetium is still the most widely available diagnostic radionuclide with optimal physical characteristics for SPECT. Although ^{18}F-labeled or ^{68}Ga-labeled derivatives will be of great value for positron emission tomography with advantages in terms of sensitivity and spatial resolution, ^{99m}Tc-labeled derivatives would be more widely available and clinically applicable.

We chose c(RGDyK) as lead structure, as it has shown suitable properties when derivatized with DTPA and labeled with ^{111}In [13]. Derivatization with HYNIC at lysine residue allowed selective labeling with ^{99m}Tc. We have recently used EDDA as coligand in the labeling of HYNIC, showing advantages over other coligands in terms of peptide labeling [14]. Using a tricine exchange labeling approach [15], high and reproducible labeling yields were achieved. Confirming previous findings, EDDA as coligand showed considerable advantages over tricine as a coligand for labeling HYNIC-RGD especially concerning lower values of plasma protein binding. We also tested two ternary coligand systems using tricine and a monodentate ligand, a triphenylphosphine (TPPTS) and a pyridine derivative (NA). Radiolabeling yields were quantitative (>99%); however, in some cases, residual amounts of [^{99m}Tc]tricine/HYNIC-RGD were detected. For both compounds, protein binding, compared to tricine alone, reached levels almost as low as that with EDDA as coligand. Especially [^{99m}Tc]tricine–TPPTS/HYNIC-RGD showed a very high hydrophilicity, with a log P of <-4.

Although HYNIC cannot be considered as an optimal ligand for the $Tc(CO)_3$ core, the labeling of HYNIC-RGD resulted in high labeling yields. However, multiple species with higher lipophilicity, compared to the method using coligands and high plasma protein binding, was observed; therefore, this radiolabeling route was not further pursued.

HYNIC-RGD showed retained binding affinity to the receptor compared to a standard monomeric RGD peptide [c(RGDfV)] and, when radiolabeled, specific binding and internalization in $\alpha_v\beta_3$-receptor-expressing cells. Comparing various stable coligand systems, EDDA showed cellular uptake higher than those of both tricine–TPPTS and tricine–NA ternary coligand systems. The differences between these coligand systems seem to be not very pronounced in vitro, however, based on these findings [^{99m}Tc]EDDA/HYNIC-RGD was selected for further in vivo evaluation.

A tumor model [^{99m}Tc]EDDA/HYNIC-RGD revealed high uptake in $\alpha_v\beta_3$-receptor-positive and low uptake in negative tumor xenografts, proofing specific receptor-mediated uptake in vivo. The same model has also been used in the development of glycosylated RGD derivatives [16], of which [^{18}F]Galacto-RGD has been successfully used to visualize $\alpha_v\beta_3$ integrin expression in patients. Fig. 6 compares the tumor-to-organ ratios (1 h postinjection) of these two compounds. Whereas tumor-to-organ ratios of [^{99m}Tc]EDDA–HYNIC-RGD were lower for the blood, heart and intestines, comparable values were found for the liver, kidneys and muscle. Considering the importance of low intestinal excretion and low kidney retention for radiolabeled peptides for diagnostic purposes, these results seem to be promising in relation to the only RGD peptide evaluated extensively in human studies so far. These data were confirmed using an alternative small cell lung cancer

model showing very similar pharmacokinetics with predominant renal excretion and low retention in the liver, blood and muscle, as well as comparable lower tumor uptake values. Imaging studies proved the receptor-mediated tumor uptake in this model.

In addition, other groups have reported on HYNIC-derivatized RGD peptide analogues for labeling with ^{99m}Tc. Early attempts using direct ^{99m}Tc labeling approaches were reported without showing specific in vivo uptake [17,18]. An attempt to use an N_3S-type ligand for labeling a cyclic RGD monomer resulted in a ^{99m}Tc-labeled peptide with receptor-mediated tumor uptake but suboptimal pharmacokinetics with especially very high kidney uptake and retention [19].

Su et al. [20] used a cyclic derivative from a Phage display library. They only found moderate tumor uptake, but could not prove specific $\alpha_v\beta_3$-mediated accumulation, possibly related to the low affinity of their peptide [21]. However, they found improvement in terms of protein binding when using EDDA instead of tricine as coligand [22]. Janssen et al. [23] used HYNIC-c(RGDfK), an analogue closely related to our tracer. For radiolabeling, they applied the ternary ligand approach, with TPPTS as monodentate ternary ligand. No in vitro data concerning cell uptake or any comparative data with other coligands were provided, in contrast to our study where EDDA as a coligand showed the highest internalization values of different coligand systems. They found high tumor uptake in a human ovarian cancer (OVCAR3) tumor model and compared the monomeric derivative with a dimeric analogue. Although tumor-to-organ ratios were superior for the monomer, they described advantages of the dimer due to higher tumor uptake and retention. However, they failed to show any specific tumor uptake in any of their models (i.e., by using blocking experiments, receptor-negative control tumors or control peptides without receptor affinity). In our study, we demonstrated specific receptor-mediated uptake of [^{99m}T]EDDA/HYNIC-RGD in a murine tumor model with $\alpha_v\beta_3$-receptor-positive and $\alpha_v\beta_3$-receptor-negative tumors. Considering the higher kidney retention of the c(RGDyK) dimer in comparison with the monomer, we see advantages of [^{99m}T]EDDA/HYNIC-RGDyK.

Summarizing these promising properties, we consider [^{99m}T]EDDA/HYNIC-RGD as a good candidate for imaging $\alpha_v\beta_3$ integrin receptor expression in tumors and tumor-induced angiogenesis. Recent data using [^{18}F]Galacto-RGD showed that $\alpha_v\beta_3$ integrin receptor expression can be visualized using noninvasive nuclear imaging techniques in vivo [24].

However, also other clinical applications may be of interest. Recently, the imaging of integrin $\alpha_v\beta_3$ in coronary arterial and peripheral vascular angiogenesis and the monitoring of its treatment using radiolabeled RGD peptides have been suggested to have important clinical potential [25]. A ^{99m}Tc-labeled RGD analogue has been used successfully for noninvasive serial "hot-spot" imaging of angiogenesis induced by ischemia [26]. In addition, other applications seem to be clinically interesting (e.g., inflammatory processes inducing angiogenesis with concomitant $\alpha_v\beta_3$ overexpression might be a useful application for radiolabeled RGD peptides) [27]. Clinical studies with this compound should reveal the true potential of this new ^{99m}Tc-labeled peptide.

Acknowledgments

This work was part of an IAEA (International Atomic Energy Agency)-coordinated research project "Development of Tc-99m-Based Small Biomolecules Using Novel ^{99m}Tc Cores". Special thanks go to Drs. D.V.S. Narasimhan and M.R.A. Pillai (Department of Nuclear Sciences and Applications, IAEA) for their considerable effort into the success of this coordinated research project. We thank Dr. D.A. Cheresh (The Scripps Research Institute, La Jolla, CA) for supplying the M21 and M21L cells.

We thank Stephan Schwarz and Misley Wambrug Altanes for their excellent technical assistance, and Prof. Irene Virgolini for her support.

References

[1] Riccabona G, Decristoforo C. Peptide targeted imaging of cancer. Cancer Biother Radiopharm 2003;18:675–87.
[2] Heppeler A, Froidevaux S, Eberle AN, Maecke HR. Receptor targeting for tumour localisation and therapy with radiopeptides. Curr Med Chem 2000;7:971–94.
[3] Reubi JC. Peptide receptors as molecular targets for cancer diagnosis and therapy. Endocr Rev 2003;24:389–427.
[4] Haubner R, Wester HJ. Radiolabeled tracers for imaging of tumour angiogenesis and evaluation of anti-angiogenic therapies. Curr Pharm Des 2004;10:1439–55.
[5] Haubner R. $\alpha_i\beta_3$-Integrin imaging: a new approach to characterize angiogenesis? Eur J Nucl Med Mol Imaging 2006;33(Suppl 13): 54–63.
[6] Felding-Habermann B, Mueller BM, Romerdahl CA, Cheresh DA. Involvement of integrin alpha V gene expression in human melanoma tumourigenicity. J Clin Invest 1992;89:2018–22.
[7] Aumailley M, Gurrath M, Muller G, Calvete J, Timpl R, Kessler H. Arg–Gly–Asp constrained within cyclic pentapeptides. Strong and selective inhibitors of cell adhesion to vitronectin and laminin fragment P1. FEBS Lett 1991;291:50–4.
[8] Haubner R, Wester HJ, Reuning U, Senekowitsch-Schmidtke R, Diefenbach B, Kessler H, et al. Radiolabeled alpha(v)beta$_3$ integrin antagonists: a new class of tracers for tumour targeting. J Nucl Med 1999;40:1061–71.
[9] Haubner R, Weber WA, Beer AJ, Vabuliene E, Reim D, Sarbia M, et al. Noninvasive visualization of the activated alpha$_v$beta$_3$ integrin in cancer patients by positron emission tomography and [^{18}F]galacto-RGD. PLoS Med 2005;2:29.
[10] Liu S, Edwards DS. ^{99m}Tc-labeled small peptides as diagnostic radiopharmaceuticals. Chem Rev 1999;99:2235–68.
[11] Decristoforo C, Melendez-Alafort L, Sosabowski JK, Mather SJ. ^{99m}Tc-HYNIC-[Tyr^3]-octreotide for imaging SST-receptor positive tumours, preclinical evaluation and comparison with ^{111}In-octreotide. J Nucl Med 2000;41:1114–9.
[12] von Guggenberg E, Behe M, Behr TM, Saurer M, Seppi T, Decristoforo C. ^{99m}Tc-labeling and in vitro and in vivo evaluation of HYNIC- and (*N* alpha-His)acetic acid-modified [D-Glu1]-minigastrin. Bioconjug Chem 2004;15:864–71.

[13] van Hagen PM, Breeman WA, Bernard HF, Schaar M, Mooij CM, Srinivasan A, et al. Evaluation of a radiolabelled cyclic DTPA-RGD analogue for tumour imaging and radionuclide therapy. Int J Cancer 2000;90:186–98.

[14] Decristoforo C, Mather SJ. 99m-Technetium labelled peptide–HYNIC conjugates. The effects of lipophilicity and stability on biodistribution. Nucl Med Biol 1999;26:389–96.

[15] Von Guggenberg E, Sarg B, Lindner H, Melendez L, Alafort SJ, Mather R, et al. Preparation via coligand exchange and characterisation of [^{99m}Tc-EDDA-HYNIC-D-Phe^{1}, Tyr^{3}]Octreotide (^{99m}Tc-EDDA/HYNIC-TOC). J Lab Comp Radiopharm 2003;46: 307–18.

[16] Haubner R, Wester HJ, Weber WA, Mang C, Ziegler SI, Goodman SL, et al. Noninvasive imaging of alpha(v)beta$_3$ integrin expression using ^{18}F-labeled RGD-containing glycopeptide and positron emission tomography. Cancer Res 2001;61:1781–5.

[17] Sivolapenko GB, Skarlos D, Pectasides D, Stathopoulou E, Milonakis A, Sirmalis G, et al. Related imaging of metastatic melanoma utilising a technetium-99m labelled RGD-containing synthetic peptide. Eur J Nucl Med 1998;25:1383–9.

[18] Noiri E, Goligorsky MS, Wang GJ, Wang J, Cabahug CJ, Sharma S, et al. Biodistribution and clearance of ^{99m}Tc-labeled Arg–Gly–Asp (RGD) peptide in rats with ischemic acute renal failure. J Am Soc Nephrol 1996;7:2682–8.

[19] Haubner R, Bruchertseifer F, Bock M, Kessler H, Schwaiger M, Wester HJ. Synthesis and biological evaluation of a (99m)Tc-labelled cyclic RGD peptide for imaging the alpha$_v$beta$_3$ expression. Nuklearmedizin 2004;43:26–32.

[20] Su ZF, Liu G, Gupta S, Zhu Z, Rusckowski M, Hnatowich DJ. In vitro and in vivo evaluation of a technetium-99m-labeled cyclic RGD peptide as a specific marker of alpha(V)beta(3) integrin for tumour imaging. Bioconjug Chem 2002;13:561–70.

[21] Weber W, Haubner R. Comment on "In vitro and in vivo evaluation of a technetium-99m-labeled cyclic RGD peptide as a specific marker of alpha$_V$beta$_3$ integrin for tumour imaging". Bioconjug Chem 2003; 14:274.

[22] Su ZF, He J, Rusckowski M, Hnatowich DJ. In vitro cell studies of technetium-99m labeled RGD-HYNIC peptide, a comparison of tricine and EDDA as co-ligands. Nucl Med Biol 2003;30:141–9.

[23] Janssen M, Oyen WJ, Massuger LF, Frielink C, Dijkgraaf I, Edwards DS, et al. Comparison of a monomeric and dimeric radiolabeled RGD-peptide for tumour targeting. Cancer Biother Radiopharm 2002;17: 641–6.

[24] Beer AJ, Haubner R, Goebel M, Luderschmidt S, Spilker ME, Wester HJ, et al. Biodistribution and pharmacokinetics of the alpha$_v$beta$_3$-selective tracer ^{18}F-galacto-RGD in cancer patients. J Nucl Med 2005; 46:1333–41.

[25] Villanueva FS. Molecular images of neovascularization: art for art's sake or form with a function? Circulation 2005;111:3188–91.

[26] Hua J, Dobrucki LW, Sadeghi MM, Zhang J, Bourke BN, Cavaliere P, et al. Noninvasive imaging of angiogenesis with a ^{99m}Tc-labeled peptide targeted at $\alpha_v\beta_3$ integrin after murine hindlimb ischemia. Circulation 2005;111:3255–60.

[27] Pichler BJ, Kneilling M, Haubner R, Braumuller H, Schwaiger M, Rocken M, et al. Imaging of delayed-type hypersensitivity reaction by PET and ^{18}F-galacto-RGD. J Nucl Med 2005;46:184–9.

New Peptide Based Freeze-Dried Kit [^{99m}Tc-HYNIC]-UBI 29-41 as a Human Specific Infection Imaging Agent

Original Article

Mostafa Gandomkar, PhD; Reza Najafi, PhD; Mohammad Mazidi; Mostafa Goudarzi; Seyed Hassan Mirfallah

[1]Nuclear Science Research School, Nuclear Science & Technology Research Institute (NSTRI), Atomic Energy Organization of Iran, Tehran, Iran

(Received 30 August 2008, Revised 29 September 2008, Accepted 5 October 2008)

ABSTRACT

Introduction: Ubiquicidin 29-41 (UBI) is a fragment of the cationic antimicrobial peptide that is present in various species including humans. The purpose of this study was to investigate radiochemical and biological characteristics of [6-hydrazinopyridine-3-carboxylic acid (HYNIC)]-UBI 29-41 designed for the labeling with ^{99m}Tc using tricine as coligand.

Methods: Synthesis was preformed on a solid phase using a standard Fmoc strategy and HYNIC precursor coupled at the N-terminus. Purified peptide conjugate was labeled with ^{99m}Tc at 100°C for 10 min. Radiochemical analysis involved ITLC and high-performance liquid chromatography methods. Peptide conjugate stability and affinity to human serum was challenged for 24 hours and its in vitro binding to bacteria was assessed. Biodistribution and accumulation of radiopeptide in *staphylococcus aureus* infected mice were studied using scintigraphy and *ex vivo* counting.

Results: Radiolabeling was performed at high specific activities, and radiochemical purity was >95%. The stability of radiolabeled peptide in human serum was excellent. *In vitro* studies showed 70% of radioactivity was bound to bacteria. After injection into mice with a bacterial infection, removing from the circulation occurred mainly by renal clearance and site of infection was rapidly detected within 30 min. Target to nontarget muscle ratio was 2.099 ± 0.05% at 30 min post injection.

Conclusion: [^{99m}Tc-HYNIC]-UBI 29-41 showed favorable radiochemical and biological characteristics which permitted detection of the infection with optimal visualization within 30 min.

Key Words: Antimicrobial peptide; HYNIC; Kit; Ubiquicidin

Iran J Nucl Med 2008; 16(1): 25-30

Corresponding author: Dr Mostafa Gandomkar, Nuclear Science Research School, Nuclear Science & Technology Research Institute (NSTRI), Atomic Energy Organization of Iran, North Karegar Ave, P.O. Box 11365-3486, Tehran, Iran.

E-mail: mgandomkar@aeoi.org.ir

INTRODUCTION

In the last decade, strong efforts have been undertaken to establish radiopeptides in nuclear medicine for receptor-specific diagnosis or therapy (1, 2). Recently, antimicrobial peptides labeled with direct or indirect methods have been proposed as new ^{99m}Tc agents to distinguish bacterial infections from sterile inflammatory processes (3-10). UBI 29-41 is a cationic human antimicrobial peptide fragment (MW 1.69 kDa) with the amino acid sequence Thr-Gly-Arg-Ala-Lys-Arg-Arg-Met-Gln-Tyr-Asn-Arg-Arg, and therefore with 6 positively charged residues and no cysteines. Many approaches have been used to radiolabel peptides with ^{99m}Tc. Usually these methods follow one of two strategies: direct or indirect labeling. It is generally thought that by direct labeling, the ^{99m}Tc is bound to sulfydryls produced by the reduction of the cysteine bridge in a peptide. Very little is known about the number of donor atoms and the coordination geometry around the ^{99m}Tc center. The indirect labeling method involves the use of a bifunctional chelating agent (BFCA) to incorporate the ^{99m}Tc into the peptide. The advantages of this labeling method include a well defined chemistry and the possibility of post conjugation labeling in which the peptide is first conjugated with a BFCA and stored until required for radiolabeling. We considered labeling of this peptide through the bifunctional chelators and among them HYNIC is more attractive because of its monodenticity that may allow the use of a variety of coligands, leading to quite different biodistributions (11, 12).

In this study, we have used a new ^{99m}Tc-labeled HYNIC-UBI 29-41 freeze-dried kit formulation for evaluation of biological activity profile and detection of infection sites in mice injected with live *S. aureus*. As a control, inflammation was induced by sterilized turpentine oil. As a difference from previous studies (9, 10), our freeze-dried kit contains a greater quantity of HYNIC-UBI 29-41 (40 µg) with some modifications in another constituent (40 µg $SnCl_2$, without adding mannitol and using acetate buffer 0.5 M, pH 4 as a solvent) and also difference in labeling procedure (100°C for 10 min).

METHODS

All chemicals were obtained from commercial sources and used without further purification. Tritylchloride resin was obtained from NovaBiochem. The prochelator HYNIC-Boc was synthesized according to Abrams et al (13). The reactive side chains of the aminoacids were masked with one of the following groups: Arg, 2,2,4,6,7-pentamethyl-dihydrobenzofurane-5-sulfonyl; Asn, triphenylmethyl; Gln, triphenylmethyl; Lys, t-butoxycarbonyl; Tyr, t-butyl; Thr, t-butyl. For sterility filtration, 20-µm Millex-GS filters from Millipore were used. Sodium pertechnetate (Na $^{99m}TcO_4$) was obtained from commercial ^{99}Mo/ ^{99m}Tc generator (Radioisotope Division, AEOI).

Analytical reverse phase-high performance liquid chromatography (RP-HPLC) was performed on a JASCO 880-PU intelligent pump HPLC system equipped with a multiwavelength detector and a flow-through Raytest-Gabi γ-detector. CC250/4 Nucleosil 120-3C18 column from Macherey-Nagel were used for HPLC. The gradient systems consisted of 0.1% trifluoroacetic acid (TFA)/water (solvent A), acetonitrile (solvent B), flow: 0.75 mL/min, λ = 280 nm. Quantitative gamma counting was performed on ORTEC Model 4001 M γ-system well counter.

Synthesis

The peptide was synthesized by standard Fmoc solid-phase synthesis on tritylchloride resin with substitution of 0.8 mmol /g. Coupling of each amino acid was performed in the presence of 3 molar excess of Fmoc-amino acid, 3 molar excess of *N*-hydroxybenzotriazole (HOBT), 3 molar excess of diisopropylcarbodiimide (DIC), and 5 molar excess of *N*-etthyldiisopropylamine (DIPEA) in *N*-methylpyrrolidone (NMP) for 2 h. Completeness of coupling reactions was monitored by the Kaiser test and the Fmoc groups were removed by adding 20% piperidine/*N*,*N*-dimethylformamide (DMF). The fully protected peptide was cleaved from the resin with 20% acetic acid. 1.2 mol HYNIC-Boc was coupled with 1.2 molar of O-(7-azabenzotriazol-1-yl)-1, 1,3,3,tetramethyluronium hexafluorophosphate (HATU) to the N-terminus of peptide. After deprotection and precipitation, product was purified and characterized by RP-HPLC and ESI-MS.

Kit formulation

1 mL solution of sodium acetate buffer 0.5 M with the final pH 4, containing 20 mg tricine, 40 µg $SnCl_2$ (20 µL of 2 mg/mL $SnCl_2$, $2H_2O$ in nitrogen purged 0.1 M HCl) and 40 µg purified HYNIC-peptide conjugate, was filtrated into a glass vial and freeze dried.

Labeling and quality control

Radiolabeling of kit was performed by adding 0.5 mL 0.9% saline in an evacuated vial and the mixtures were allowed to preincubate for 5 min. Afterwards 555 MBq $^{99m}TcO_4^-$ in 0.5 mL saline was added to the vial and incubated for 10 min at 100ºC. After cooling to

room temperature, the labeled peptide was analyzed by analytical HPLC and ITLC on silica gel 60 (Merck) using different mobile phases. 2-Butanone for free $^{99m}TcO_4^-$ (R_f = 1), 0.1 M sodium citrate pH 5 to determine the nonpeptide-bound ^{99m}Tc coligand with $^{99m}TcO_4^-$ (R_f = 1) and methanol/1 M ammonium acetate 1/1 for ^{99m}Tc- colloid (R_f = 0).

Stability and affinity to human serum

The stability and affinity of [^{99m}Tc-HYNIC]-UBI 29-41 was challenged by adding 1 ml of radiolabeled peptide with activity between 10 and 20 mCi to a vial contain 1ml fresh human serum. The reaction mixtures were incubated at 37°C for 24 h and analyzed by ITLC for stability and placing 100 µl of reaction mixture on a PD10 column to evaluate affinity to plasma proteins. After washing the column with PBS contain 0.1% BSA activity bound to serum protein and labeled peptide was measured with well-type gamma counter.

In vitro binding assay

Over night cultures of *S. aureus* were prepared in brain-heart infusion broth (Oxoid, Basingstoke, UK) in a shaking water-bath at 37°C. The next day, bacteria were washed, counted, aseptically aliquoted at a concentration of 1×10^8 colony forming units (CFU)/mL, stored at -20°C and thawed immediately before use. Binding of ^{99m}Tc-labeled peptide to bacteria was assessed at 4°C. In short, 0.1 mL of 15 mM sodium phosphate buffer (Na-PB, pH 7.5) containing 1/10 of the preparation containing labeled peptide was transferred to an Eppendorf vial. Next, 0.8 mL of 50% (v/v) of 0.01 M acetic acid in Na-PB containing 0.01% (v/v) Tween-80 and 0.1 mL of Na-PB containing approximately 2×10^7 viable bacteria were added. The mixture, with a final pH of 5, was incubated for 1 h at 4°C and thereafter the vials were centrifuged in a pre-cooled centrifuge at 2,000 × *g* for 5 min. The supernatant was removed and the bacterial pellet was gently resuspended in 1 mL of Na-PB and re-centrifuged as above. The supernatant was removed and the radioactivity in the bacterial pellet was determined in a dose calibrator. The radioactivity associated with bacteria was expressed as percentage of added ^{99m}Tc activity bound to 2×10^7 of viable bacteria.

Animal Studies

Male Swiss mice, weighting 25-30 g were infected by injecting 0.1 mL of saline containing 2×10^7 CFU bacteria into right thigh muscle. After 18 h rats were injected under ether anesthesia with 20 MBq of 0.35 nmol [^{99m}Tc-HYNIC]-UBI 29-41, in saline into the tail vein. For comparison, a sterile inflammation was induced by an intramuscular injection of 0.1 mL of sterile saline containing 100 µg of turpentine oil 24 h preceding administrations of the tracers. At 1 h after injection, accumulation of the tracer in infected or inflamed areas was assessed by planer scintigraphy under ether anesthesia. For ex vivo counting's, mice's were sacrificed after 30 min, 1 and 2 h, and organs of interest were collected, weighed and radioactivity was measured in a γ-counter.

RESULTS

Synthesis and radiolabeling

After standard solid-phase synthesis of the peptide, coupling of HYNIC-Boc to the N-terminus of peptide was performed in the solution in an overall yield of 40% (Fig. 1).

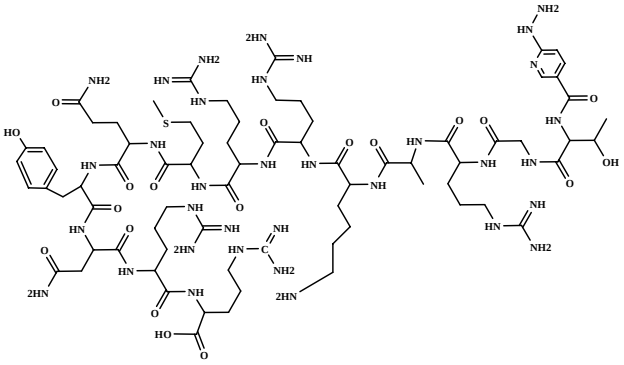

Fig. 1: Structural formulae of [HYNIC]-UBI 29-41

The composition and structural identity of [HYNIC]-UBI 29-41 were verified by analytic HPLC and ESI-MS (Fig. 2, 3).

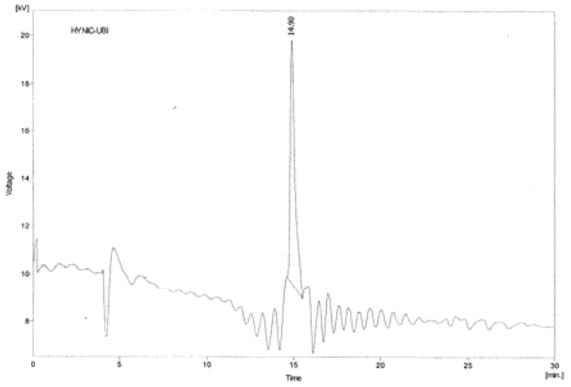

Fig. 2: RP-HPLC analysis of [HYNIC]-UBI 29-41

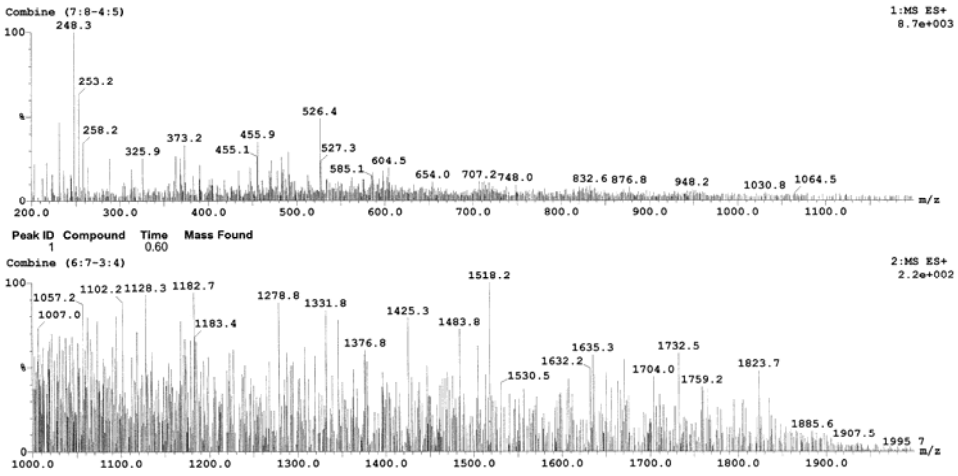

Fig. 3: Mass spectrometric analysis of [HYNIC]-UBI 29-41

Table 1: Biodistribution in mice with thigh muscle infection after injection of [^{99m}Tc-HYNIC]-UBI 29-41. Data are presented as %ID/g±SD and results are the means of groups of four animals.

Organ	Time		
	30 min	1 h	2 h
Blood	1.01 ± 0.07	0.91 ± 0.04	0.81 ± 0.02
Urine	1.39 ± 0.22	2.33 ± 0.23	3.11 ± 0.32
Kidney	35.69 ± 14.30	30.13 ± 10.20	22.06 ± 6.03
Gut	1.89 ± 0.92	1.68 ± 0.06	1.10 ± 0.01
Spleen	0.66 ± 0.07	0.78 ± 0.04	0.79 ± 0.02
Stomach	2.90 ± 0.39	1.66 ± 0.04	1.09 ± 0.01
Intestine	0.85 ± 0.22	0.60 ± 0.11	0.49 ± 0.02
Liver	1.44 ± 0.01	1.32 ± 0.01	1.15 ± 0.03
Lung	1.13 ± 0.20	1.11 ± 0.02	0.92 ± 0.02
Heart	0.76 ± 0.09	0.54 ± 0.05	0.24 ± 0.03
Infected muscle	0.93 ± 0.09*	1.05 ± 0.02*	0.71 ± 0.05*
Non-infected muscle	0.45 ± 0.01	0.51 ± 0.25	0.42 ± 0.02
Infection/non-infection ratio	2.099 ± 0.05	2.051 ± 0.14	1.69 ± 0.04

* $P < 0.05$ vs. Non-infected muscle.

The purity was >97%, as confirmed by the HPLC method. The labeling yield of [^{99m}Tc-HYNIC]-UBI 29-41 was >95%, acquired via HPLC and also ITLC at a specific activity of 50 GBq/μmol that was stable for 24 hours. The HPLC elution times were 5.03 min for $^{99m}TcO_4^-$ and 15.54 min for ^{99m}Tc peptide (Fig. 4).

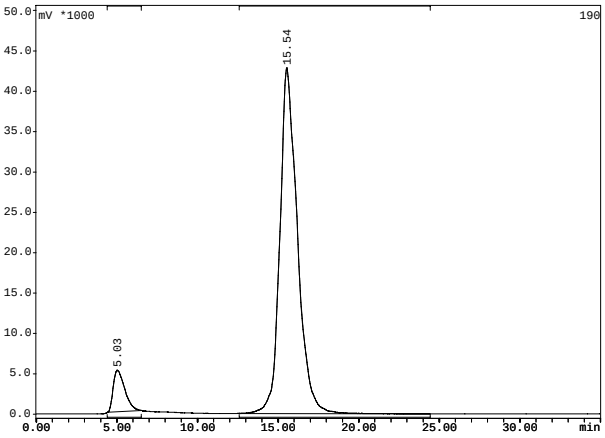

Fig. 4: RP-HPLC analysis of [^{99m}Tc-HYNIC]-UBI 29-41

Stability, affinity and binding assay

The affinity of the labeled peptide to human serum proteins after 24 hour was less than 25±5%. Labeled peptide was stable in plasma with radiochemical purity of more than 90% after 24 h incubation. In vitro testing of [^{99m}Tc-HYNIC]-UBI 29-41 to *S. aureus* showed 75% of radioactivity bound to bacteria. In additional experiments we observed a significantly decrease by 60% in the binding to bacteria that had been pre-exposed for 1 h at 4^{o}C with a 100 molar excess of [HYNIC]-UBI 29-41 peptide.

Animal biodistribution

The results of biodistribution in mice with *S. aureus* thigh muscle infection are summarized in Table 1. The radioligand displayed a rapid blood clearance mainly through the kidneys and subsequently the urinary bladder. Small amount of radioactivity were observed in the liver, spleen and thyroids. Accumulation of radiopeptide in the infected thigh muscles as indicated by a T/NT ratio was 2.099 ± 0.05% at 30 min after injection.

Typical Scintigrams of mice's with thigh muscle infection our inflammation and normal at 60 min after injection of radiopeptide are shown in Fig 5. High uptakes of activity in infection site with no accumulation in inflamed site were observed. Upon autopsy the bacterial infection had the same appearance as demonstrated on the scintigraphic image.

DISCUSSION

It should be realized that Ubiquicidin 29-41 can be labeled rapidly with high yields with ^{99m}Tc using a direct or indirect labeling technique (5-10). Unfortunately, the mechanisms underlying the direct labeling of peptides with ^{99m}Tc are not well understood (5). This may be a drawback for the development of a kit based on the Ubiquicidin 29-41. Therefore, we considered the possibility of radiolabeling peptides through the intermediacy of a HYNIC as a chelator, prepared from lyophilized kit based on new formulation.

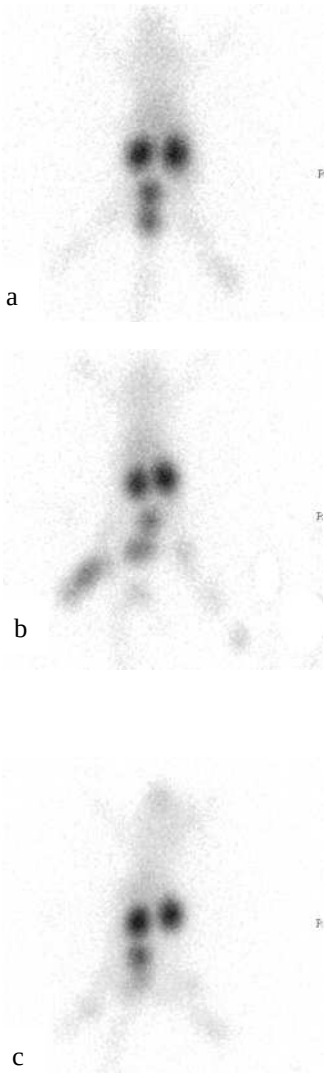

Fig. 5: Typical scintigrams of normal mice's (a), with thigh muscle infection (b) and inflammation (c) at 60 min after injection of [^{99m}Tc-HYNIC]-UBI 29-41.

The ^{99m}Tc labeling was straightforward for kit formulation with high radiochemical yields (>95%)

and specific activities of about 50 GBq/μmol. The present results revealed that [^{99m}Tc-HYNIC]-UBI 29-41 preferentially bind to bacteria. It should be kept in mind that in our *in vitro* competition assays we observed inhibition of binding of [^{99m}Tc-HYNIC]-UBI 29-41 to *S. aureus* by unlabeled [HYNIC]-UBI 29–41 with maximal inhibition of approximately 60% when 100-fold excess of unlabeled peptide was used as competitor. Since the conditions of our *in vitro* competition assay do not represent the physiological texture at the site of infection, we cannot assume that a peptide would be successful at infection imaging on the basis of good *in vitro* binding to bacteria.

The biodistribution of radiopeptide showed a good correlation between in vitro binding and accumulation in site of infection in mice. [^{99m}Tc-HYNIC]-UBI 29-41 allow rapid visualization of infections with gram-positive and gram-negative bacteria with little or no accumulation in inflamed thigh muscles, indicating that these radiopeptide directly tag the bacteria at the site of infection.

Results from our new kit formulation were comparable with those obtained by Welling et al. [9, 10]. They used the same radiopharmaceutical but prepared from wet labeling method and different kit formulation, to study its biodistribution and observed binding of 40% and T/NT ratio of 1.84 ± 0.27 (%ID/g) after 2 h compared with 75% and 1.69 ± 0.04 (%ID/g) from our kit, respectivly.

CONCLUSION

[^{99m}Tc-HYNIC]-UBI 29-41 obtained from lyophilized kit with 40 μg peptide can be used for differentiating infection compared with that of the sterile inflammatory site. The optimum time for imaging is 30 min after tracer injection.

AKNOWLEDGEMENT

The author wishes to thank H. Talebi and M. Zoghi of the radioisotope department (AEOI) for providing sodium pertechnetate and assistance in quality control tests.

REFERENCES

1. Fischman AJ, Babich JW, Strauss HW. A ticket to ride – peptide radiopharmaceuticals. J Nucl Med. 1993; 34: 2253-2263.

2. Thakur ML. Radiolabeled peptides-Now and the future. Nucl Med Commun. 1995; 16: 724-732.

3. Welling M, Paulusma-Annema A, Balter HS, Pauwels EKJ, Nibbering PH. Technetium-99m labeled antimicrobial peptides discriminate between bacterial infections and sterile inflammations. Eur J Nucl Med. 2000; 27: 291-301.

4. Nibbering PH, Welling M, Van Den Broek, Pauwels EKJ. Radiolabelled antimicrobial peptides for imaging of infections: a review. Nucl Med Commun. 1998; 19: 1117-1121.

5. Welling M, Monguera S, Lupetti A, Balter HS, Bonetto V, Mazzi U, et al. Radiochemical and biological characteristics of ^{99m}Tc-UBI 29-41 for imaging of bacterial infections. Nucl Med Biol. 2002; 29: 413-422.

6. Ferro-Flores G, Arteaga de Murphy C, Pedraza-Lopez M, Melendez-Alafort L, Zhang YM, Rusckowski M, et al. In vitro and in vivo assessment of ^{99m}Tc-UBI specificity for bacteria. Nucl Med Biol 2003; 30: 597-603.

7. Welling MM, Lupetti A, Balter HS, Lanzzeri S, Souto B, Rey AM, et al. ^{99m}Tc labeled antimicrobial peptides for detection of bacterial and *Candida albicans* infections. J Nucl Med 2001; 42: 788-794.

8. Lupetti A, Welling MM, Pauwels EKJ, Nibbering PH. Radiolabelled antimicrobial peptides for infection detection. Lancet Infect Dis. 2003; 3: 223-229.

9. Welling MM, Visentin R, Feitsma HI, Lupetti A, Pauwels EK, Nibbering PH. Infection detection in mice using ^{99m}Tc-labeled HYNIC and N2S2 chelate conjugated to the antimicrobial peptide UBI 29-41. Nucl Med Biol 2004; 31: 503-9.

10. Welling MM, Korsak A, Gorska B, Oliver P, Mikolajczak R, Balter HS, et al. Kit with technetium-99m labeled antimicrobial peptide UBI 29-41 for specific infection detection. J Label Compd Radiopharm 2005; 48: 683-691.

11. Decristoforo C, Melendez-Alafort L, Sosabowski JK, Mather SJ. ^{99m}Tc-HYNIC-[Tyr^3]-octreotide for imaging somatostatin-receptor-positive tumors: preclinical evaluation and comparison with ^{111}In-octreotide. J Nucl Med. 2000; 41: 1114-1119.

12. Babich JW, Fischman AJ. Effect of "co-ligand" on the biodistribution of ^{99m}Tc-labeled hydrazino nicotinic acid derivatized chemotactic peptides. Nucl Med Biol. 1995; 22: 25-30.

13. Abrams MJ, Juweid M, tenKate CI, Schwartz DA, Hauser MM, Gaul FE, et al. Technetium-99m-human polyclonal IgG radiolabeled via the hydrazino nicotinamide derivative for imaging focal sites of infection in rats. J Nucl Med. 1990; 31: 2022-2028.